Electronic Supplementary Material (ESI) for Dalton Transactions.

Electronic Supplementary Information

Successive Syntheses and Magnetic Research of Homodinuclear Lanthanide Macrocyclic Complexes †

Xiang Li, Yu-Han Liu, Guang-Zhou Zhu, Feng-Lei Yang,* and Feng Gao*

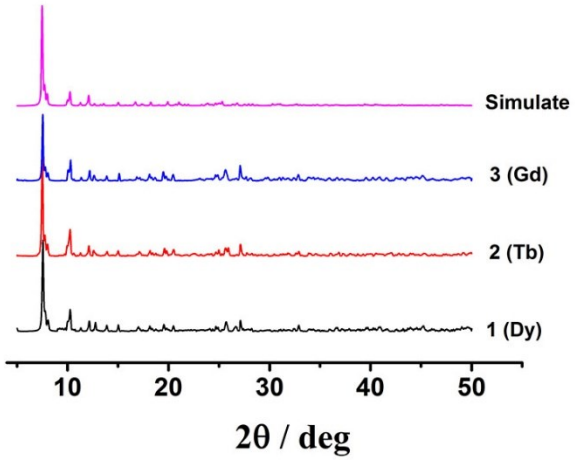

Fig. S1 Experimental and simulated PXRD patterns of complexes **1**–**3**.

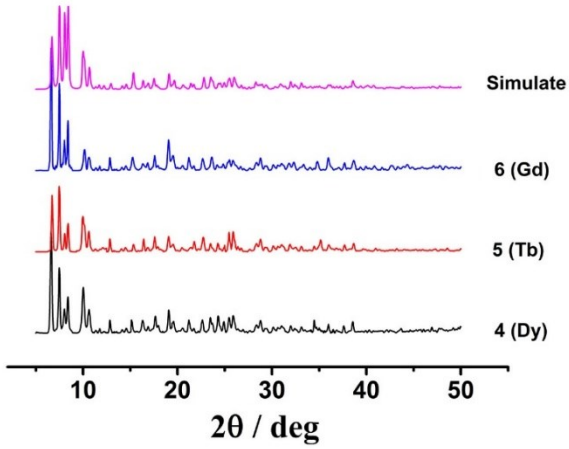

Fig. S2 Experimental and simulated PXRD patterns of complexes **4**–**6**.

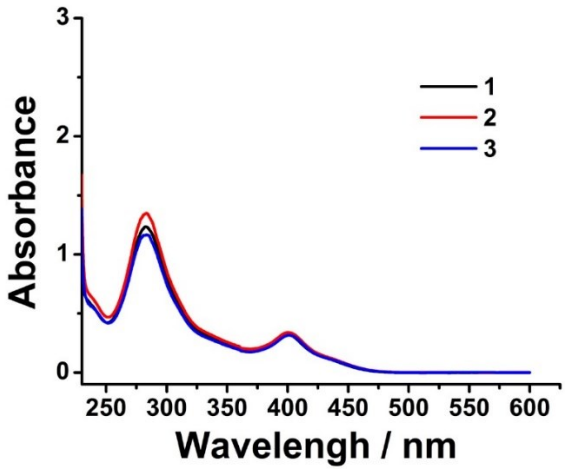

Fig. S3 UV-Vis absorption spectra for complexes **1**–**3** in dichloromethane (c = 1 × 10^{-5} M).

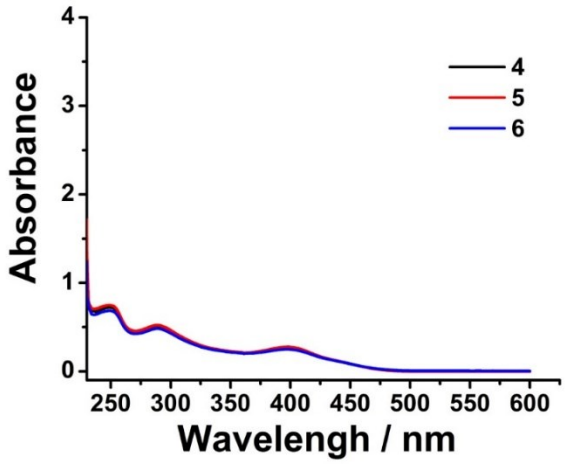

Fig. S4 UV-Vis absorption spectra for complexes **4**–**6** in dichloromethane (c = 2 × 10^{-5} M).

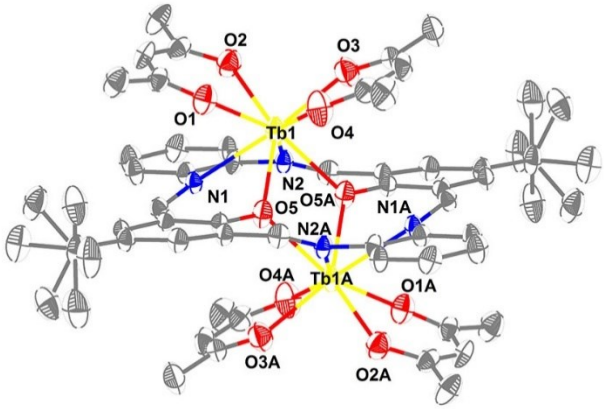

Fig. S5 Molecular structure of Tb complex **2** with hydrogen atoms omitted for clarity (Tb yellow, N blue, O red and C grey).

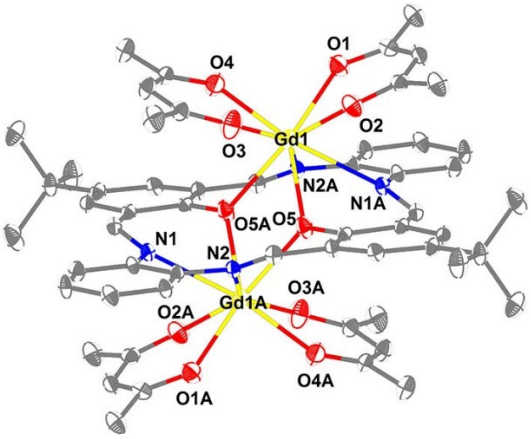

Fig. S6 Molecular structure of Gd complex **3** with hydrogen atoms omitted for clarity (Gd yellow, N blue, O red and C grey).

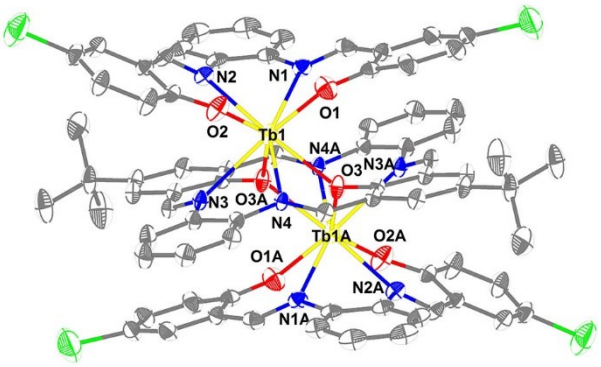

Fig. S7 Molecular structure of Tb complex **5** with hydrogen atoms omitted for clarity (Tb yellow, N blue, Cl green, O red and C grey).

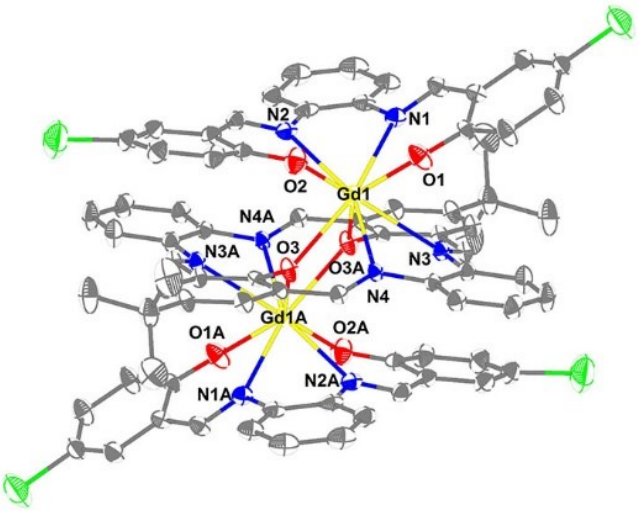

Fig. S8 Molecular structure of Gd complex **6** with hydrogen atoms omitted for clarity (Gd yellow, N blue, Cl green, O red and C grey).

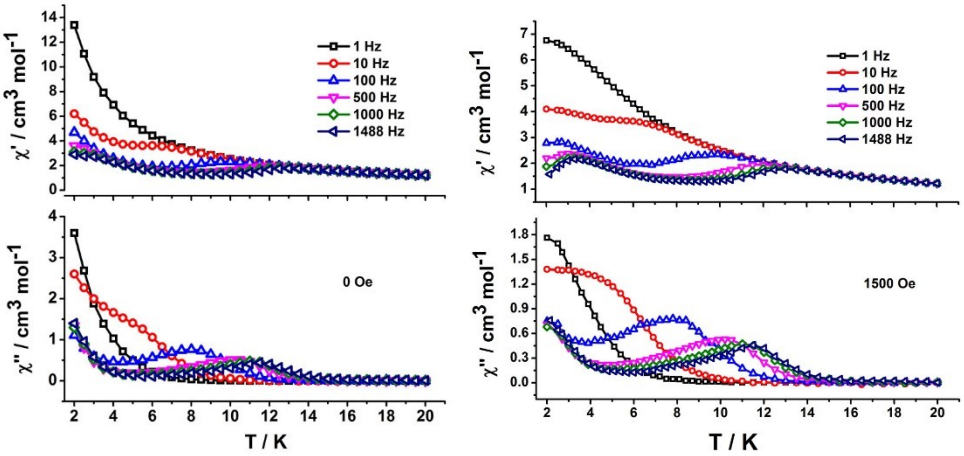

Fig. S9 Temperature-dependent in-phase (χ') and out-of-phase (χ'') ac susceptibilities of Dy complex **1** obtained at frequencies ranging from 1.0 to 1488 Hz under H_{dc} = 0 Oe (left) and H_{dc} = 1500 Oe (right), respectively.

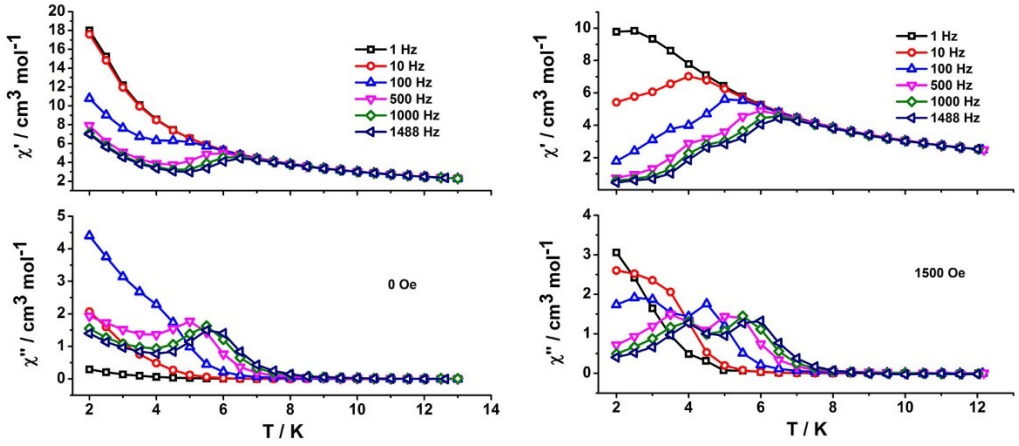

Fig. S10 Temperature-dependent in-phase (χ') and out-of-phase (χ'') ac susceptibilities of Dy complex **4** obtained at frequencies ranging from 1.0 to 1488 Hz under H_{dc} = 0 Oe (left) and H_{dc} = 1500 Oe (right), respectively.

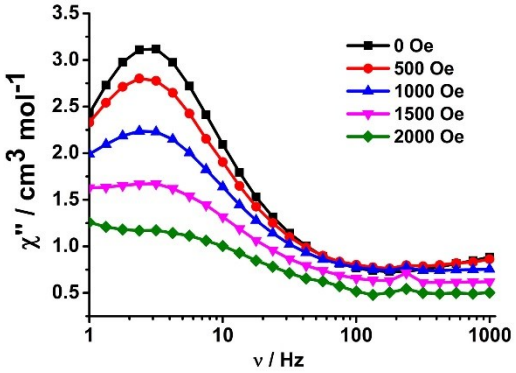

Fig. S11 Frequency-dependence out-of-phase (χ'') ac susceptibilities for Dy complex **1** at 2.5 K under different external fields.

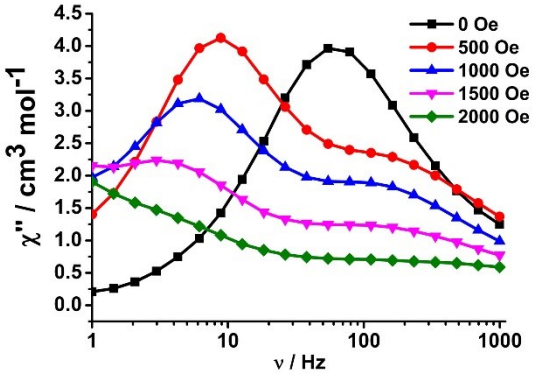

Fig. S12 Frequency-dependence out-of-phase (χ'') ac susceptibilities for Dy complex **4** at 2.5 K under different external fields.

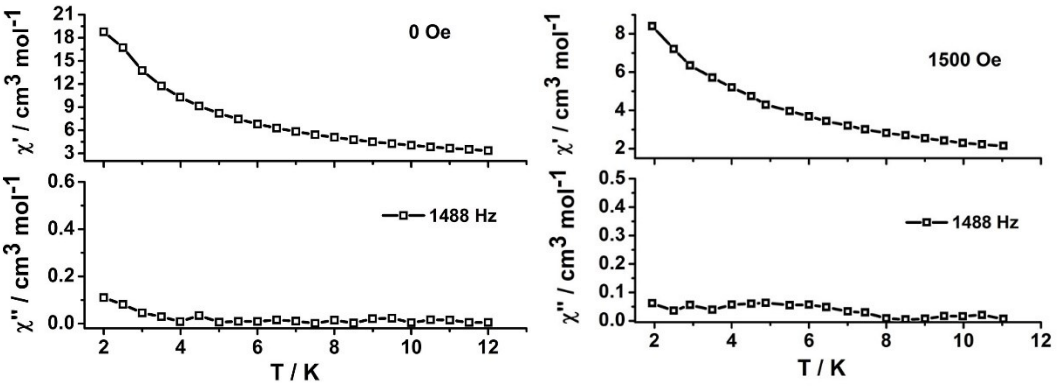

Fig. S13 Temperature-dependent in-phase (χ') and out-of-phase (χ'') ac susceptibilities of Tb complex **2** at the frequency of 1488 Hz under H_{dc} = 0 Oe (left) and H_{dc} = 1500 Oe (right), respectively.

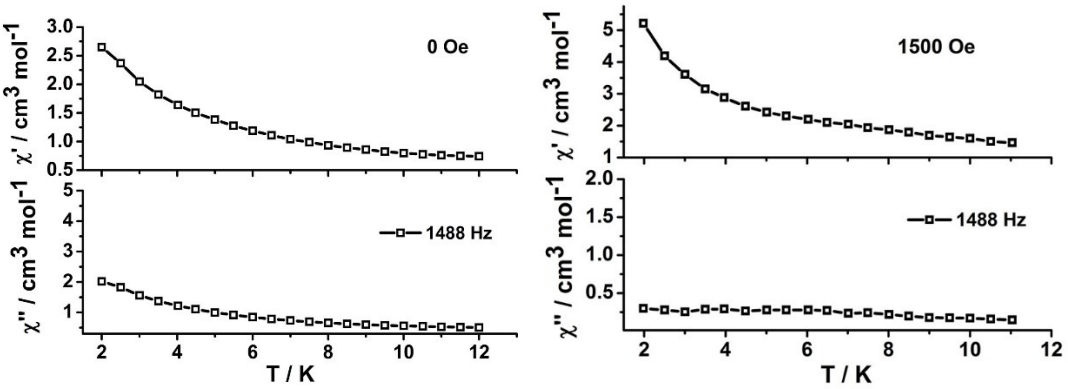

Fig. S14 Temperature-dependent in-phase (χ') and out-of-phase (χ'') ac susceptibilities of Tb complex **5** at the frequency of 1488 Hz under H_{dc} = 0 Oe (left) and H_{dc} = 1500 Oe (right), respectively.

Table S1 Selected bond lengths (Å) and angles (°) for complexes **1**-**3**.

	1 [a]	**2** [b]	**3** [c]
Ln(1)-O(1)	2.315(3)	2.347(3)	2.338(2)
Ln(1)-O(2)	2.317(3)	2.331(3)	2.355(2)
Ln(1)-O(3)	2.314(3)	2.328(3)	2.343(2)
Ln(1)-O(4)	2.335(3)	2.323(3)	2.337(2)
Ln(1)-O(5)	2.325(3)	2.311(3)	2.330(2)
Ln(1)-O(5)#1	2.303(3)	2.340(3)	2.342(2)
Ln(1)-N(1)	2.521(4)	2.562(4)	2.572(3)
Ln(1)-N(2)	2.549(4)	2.537(4)	2.552(3)
O(1)-Ln(1)-O(2)	74.37(13)	73.19(11)	73.09(8)
O(3)-Ln(1)-O(4)	73.42(12)	74.46(12)	74.01(8)
O(1)-Ln(1)-O(4)	76.34(12)	76.56(12)	79.61(8)
O(2)-Ln(1)-O(3)	78.81(12)	79.08(11)	76.99(8)
N(1)-Ln(1)-N(2)	64.30(12)	63.84(11)	63.65(8)
O(5)-Ln(1)-O(5)#1	63.72(12)	63.44(11)	63.58(8)
O(5)-Ln(1)-N(1)	68.06(11)	66.72(11)	66.43(8)
Ln(1)-O(5)-Ln(1)#1	116.28(12)	116.56(11)	116.42(8)
O(5)-Ln(1)-Ln(1)#1	31.69(7)	31.94(7)	31.69(5)

Symmetry transformations used to generate equivalent atoms: #1[a] -x+1,-y+1,-z+2; #1[b] -x+1,-y,-z; #1[c] -x+1,-y+1,-z+1.

Table S2 Selected bond lengths (Å) and angles (°) for complexes **4**-**6**.

	4 [d]	**5**[e]	**6**[f]
Ln(1)-O(1)	2.220(3)	2.242(3)	2.248(3)
Ln(1)-O(2)	2.230(3)	2.234(3)	2.259(3)
Ln(1)-O(3)	2.317(2)	2.363(2)	2.383(3)
Ln(1)-O(3)#1	2.353(2)	2.323(2)	2.335(3)
Ln(1)-N(1)	2.517(3)	2.542(3)	2.548(4)
Ln(1)-N(2)	2.526(3)	2.531(3)	2.550(4)
Ln(1)-N(3)	2.492(3)	2.533(3)	2.547(4)
Ln(1)-N(4)	2.517(3)	2.514(3)	2.527(3)
N(1)-Ln(1)-N(2)	63.84(10)	63.54(11)	63.35(13)
N(3)-Ln(1)-N(4)	65.22(10)	64.62(10)	64.31(11)
O(1)-Ln(1)-O(2)	83.43(10)	83.71(10)	84.60(12)
O(3)-Ln(1)-O(3)#1	64.29(9)	63.84(10)	63.79(11)
Ln(1)-O(3)-Ln(1)#1	115.71(9)	116.16(10)	116.21(11)

Symmetry transformations used to generate equivalent atoms: #1[d] -x,-y+1,-z+2; #1[e] -x+1,-y,-z+1; #1[f] -x,-y+2,-z.

Table S3 Summary of structural parameters for complexes **1**-**3**.

	1	**2**	**3**
Average Ln-N bond length (Å)	2.535	2.550	2.562
Average Ln-O bond length (Å)	2.318	2.331	2.342
Ln1 to O1-O2-O3-O4 plane center distance (Å)	1.152(4)	1.154(3)	1.155(3)
Ln1 to N1-N2-O5-O5A plane center distance (Å)	1.552(3)	1.572(3)	1.584(3)
Dihedral angle between O1-O2-O3-O4 and N1-N2-O5-O5A planes (°)	1.93(10)	1.64(10)	1.74(12)
Shortest intermolecular $Ln^{3+}\cdots Ln^{3+}$ distance (Å)	9.395(3)	9.410(3)	9.342(3)
Intramolecular $Ln^{3+}\cdots Ln^{3+}$ distance (Å)	3.931(4)	3.956(4)	3.971(3)

Table S4 Summary of structural parameters for complex **4**-**6**.

	4	**5**	**6**
Average Dy-N bond length (Å)	2.513	2.530	2.543
Average Dy-O bond length (Å)	2.280	2.291	2.306
Ln1 to O1-O2-N1-N2 plane center distance (Å)	1.301(4)	1.315(3)	1.322(2)
Ln1 to O3-O3A-N3-N4 plane center distance (Å)	1.530(3)	1.553(2)	1.569(3)
Dihedral angle between O1-O2-N1-N2 and O3-O3A-N3-N4 planes (°)	6.67(9)	6.58(8)	6.87(9)
Shortest intermolecular $Ln^{3+}\cdots Ln^{3+}$ distance (Å)	9.563(4)	9.551(4)	9.538(3)
Intramolecular $Ln^{3+}\cdots Ln^{3+}$ distance (Å)	3.953(5)	3.978(4)	4.006(3)

Table S5 Parameters obtained by continuous shape measurement (CShM) method for study of central Ln(III) coordination sphere of complexes **1**–**6**. (The S values indicate the proximity to the selected ideal polyhedron, S = 0 corresponds to the non-distorted polyhedron).

	1	**2**	**3**	**4**	**5**	**6**
Cube (CU, O_h)	8.901	8.929	8.861	9.677	9.716	9.826
Square antiprism (SAP, D_{4d})	0.903	0.953	0.988	1.664	1.804	1.879
Triangular dodecahedron (TDD, D_{2d})	2.670	2.714	2.707	3.142	3.191	3.200
Biaugmented trigonal prism (BTPR, C_{2v})	2.265	2.261	2.265	3.113	3.210	3.211

Table S6 Relaxation fitting parameters of the Cole-Cole plots using the generalized Debye model[a] for Dy complex **1** in the temperature range of 3.0–11.0 K under H_{dc} = 0 Oe and H_{ac} = 3.0 Oe.

T / K	χ_s / cm^3 mol^{-1}	χ_T / cm^3 mol^{-1}	ln(τ / s)	α
3.0	3.1370	10.7041	-3.0215	0.23
4.0	2.3102	7.5030	-3.4834	0.22
5.0	1.8740	5.6743	-4.0375	0.19
6.0	1.5866	4.5540	-4.7190	0.17
7.0	1.4064	3.8115	-5.4561	0.15
8.0	1.3101	3.2651	-6.1506	0.13
9.0	1.2257	2.8542	-6.8460	0.13
10.0	1.1718	2.5354	-7.5649	0.12
11.0	1.1159	2.2817	-8.4192	0.11

[a] $\chi_{total}(\omega) = \chi_S + \left[\frac{\chi_T - \chi_S}{1 + (i\omega\tau)^{1-\alpha}}\right]$

Where χ_s is the adiabatic susceptibility, χ_T is the isothermal susceptibility, ω (=2πf) is the angular frequency, τ represents the magnetization relaxation times.

Table S7 Relaxation fitting parameters of the Cole-Cole plots using the generalized Debye model for Dy complex **4** in the temperature range of 2.5–6.0 K under H_{dc} = 0 Oe and H_{ac} = 3.0 Oe.

T / K	χ_s / cm^3 mol^{-1}	χ_T / cm^3 mol^{-1}	ln(τ / s)	α
2.5	5.4555	15.4159	-6.0709	0.14
3.0	4.3924	12.2625	-6.2290	0.13
3.5	3.6953	10.1656	-6.4088	0.12
4.0	3.1937	8.6220	-6.6808	0.11
4.5	2.7966	7.4546	-7.1617	0.10
5.0	2.4636	6.5633	-7.8505	0.09
5.5	2.1179	5.8578	-8.6823	0.08
6.0	1.5075	5.2971	-9.6883	0.12

Table S8 Relaxation fitting parameters of the Cole-Cole plots using the generalized Debye model for Dy complex **1** in the temperature range of 3.6–10.5 K under H_{dc} = 1500 Oe and H_{ac} = 3.0 Oe.

T / K	χ_s / cm^3 mol^{-1}	χ_T / cm^3 mol^{-1}	ln(τ / s)	α
3.6	2.1443	7.1661	-3.3842	0.34
4.2	1.9806	6.2650	-3.7760	0.30
4.8	1.7963	5.5498	-4.1545	0.27
5.4	1.6514	4.9172	-4.5618	0.24
6.0	1.5287	4.4016	-4.9707	0.21
7.0	1.3721	3.7242	-5.6719	0.17
8.0	1.2860	3.2170	-6.3305	0.14
9.0	1.2124	2.8346	-6.9840	0.13
10.0	1.1729	2.5319	-7.6457	0.11
10.5	1.1341	2.3973	-8.0528	0.12

Table S9 Relaxation fitting parameters of the Cole-Cole plots using the generalized Debye model for Dy complex **4** in the temperature range of 2.5–6.0 K under H_{dc} = 1500 Oe and H_{ac} = 3.0 Oe.

T / K	χ_s / cm^3	χ_T / cm^3	ln(τ / s)	α
2.5	1.1100	14.5033	-3.1498	0.49
3.0	2.0681	11.7271	-3.7962	0.40
3.5	2.7883	9.6980	-4.5161	0.30
4.0	2.8824	8.2923	-5.4011	0.21
4.5	2.3746	7.4058	-6.5657	0.22
5.0	2.4403	6.6051	-7.5010	0.13
5.5	2.3321	5.9850	-8.4799	0.10
6.0	1.7472	5.4621	-9.6598	0.15

Computational details

Both of binuclear complexes **1** and **4** with central symmetrical structure have one type of magnetic center Dy^{3+} ion. Complete-active-space self-consistent field (CASSCF) calculations on individual Dy(III) fragments for **1** and **4** (see Fig. S15 for the calculated model structures of **1** and **4**) on the basis of single-crystal X-ray determined geometry have been carried out with MOLCAS 8.4[S1] program package. Each individual Dy(III) fragment in **1** and **4** was calculated keeping the experimentally determined structure of the corresponding compound while replacing the neighboring Dy(III) ion by diamagnetic Lu^{III}.

The basis sets for all atoms are atomic natural orbitals from the MOLCAS ANO-RCC library: ANO-RCC-VTZP for Dy(III); VTZ for close N and O; VDZ for distant atoms. The calculations employed the second order Douglas-Kroll-Hess Hamiltonian, where scalar relativistic contractions were taken into account in the basis set and the spin-orbit couplings were handled separately in the restricted active space state interaction (RASSI-SO) procedure. Active electrons in 7 active orbitals include all *f* electrons (CAS(9 in 7) in the CASSCF calculation. To exclude all the doubts, we calculated all the roots in the active space. We have mixed the maximum number of spin-free state which was possible with our hardware (all from 21 sextets, 128 from 224 quadruplets, 130 from 490 doublets for Dy(III). SINGLE_ANISO[S2] program was used to obtain the energy levels, ***g*** tensors, magnetic axes, *et al.* based on the above CASSCF/RASSI-SO calculations.

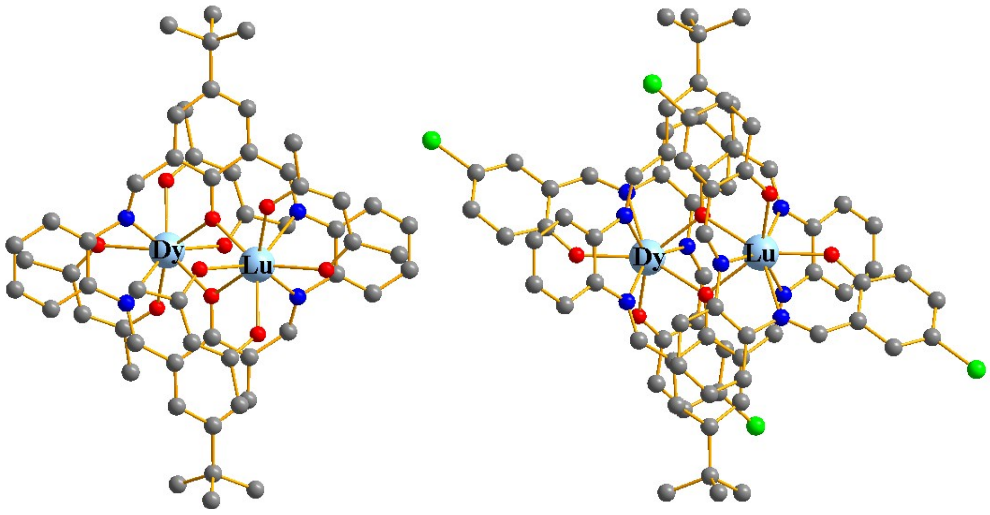

1 **4**

Fig. S15 Calculated model structures of complexes **1** and **4**; H atoms are omitted for clarify.

Table S10 Calculated energy levels (cm^{-1}), $\boldsymbol{g}$ (g_x, g_y, g_z) tensors and predominant m_J values of the lowest eight Kramers doublets (KDs) of individual Dy(III) fragments for complexes **1** and **4** using CASSCF/RASSI-SO with MOLCAS 8.4.

KDs	**1**			**4**		
	E/cm^{-1}	$\boldsymbol{g}$	m_J	E/cm^{-1}	$\boldsymbol{g}$	m_J
1	0.0	0.009 0.018 19.382	±15/2	0.0	0.019 0.078 18.199	±15/2
2	112.1	0.043 0.195 16.055	±9/2	66.9	0.069 0.129 5.977	±13/2
3	139.6	0.578 0.836 12.558	±11/2	200.3	0.506 0.728 3.069	±11/2
4	197.4	3.968 4.705 8.243	±5/2	274.5	1.657 3.330 9.818	±9/2
5	240.5	3.235 3.343 10.022	±7/2	337.4	9.713 6.063 2.205	±7/2
6	283.7	0.509 2.026 14.727	±3/2	367.9	2.537 3.003 14.499	±5/2
7	350.8	0.099 0.372 18.189	±13/2	428.2	0.263 0.655 16.657	±3/2
8	402.8	0.087 0.261 18.991	±1/2	536.4	0.014 0.054 19.388	±1/2

Table S11 Wave functions with definite projection of the total moment | m_J > for the lowest two KDs of individual Dy(III) fragments for complexes **1** and **4**.

	E/cm^{-1}	wave functions
1	0.0	92.2%|±15/2>+5.7%|±11/2>
	112.1	27.4%|±13/2>+14.8%|±7/2>+15.5%|±5/2>+15.6%|±3/2>
4	0.0	73.0%|±15/2>+14.1%|±11/2>
	66.9	36.0%|±13/2>+25.1%|±9/2>+17.4%|±7/2>+9.0%|±5/2>

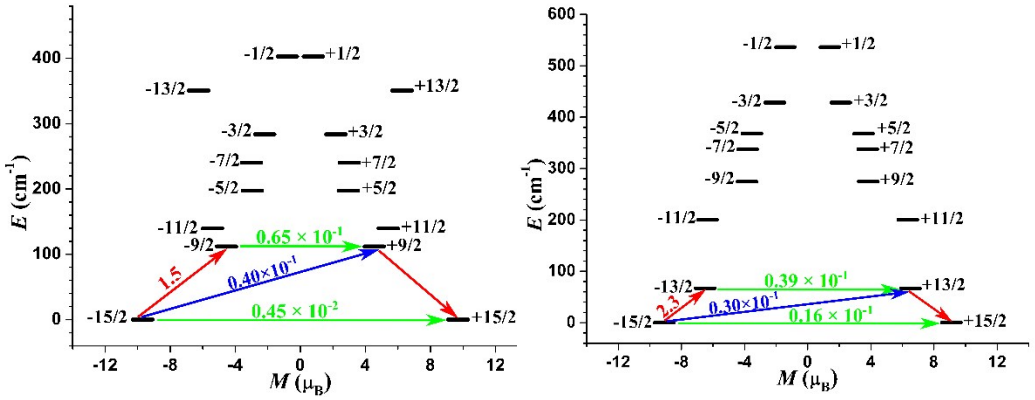

1 **4**

Fig. S16 Magnetization blocking barriers for individual Dy(III) fragments in **1** and **4**. The thick black lines represent the KDs as a function of their magnetic moment along the magnetic axis. The green lines correspond to diagonal quantum tunneling of magnetization (QTM); the blue line represent off-diagonal relaxation process. The numbers at each arrow stand for the mean absolute value of the corresponding matrix element of transition magnetic moment.

To fit the exchange interactions of complexes **1** and **4**, we took two steps to obtain them. Firstly, we calculated individual Dy(III) fragments using CASSCF/RASSI-SO to obtain the corresponding magnetic properties. Then, the exchange interactions between the magnetic centers were considered within the Lines model, while the account of the dipole-dipole magnetic couplings were treated exactly. The Lines model is effective and has been successfully used widely in the research field of *d* and *f*-elements single-molecule magnets.

For complexes **1** and **4**, there is only one type of *J*.

The Ising exchange Hamiltonian is:

$$\hat{H}_{exch} = -J_{total}\hat{S}_{Dy1}\cdot\hat{S}_{Dy2}$$

The J_{total} is the parameter of the total magnetic interaction ($J_{total} = J_{diploar} + J_{exchange}$) between magnetic center ions. The $\hat{S}_{Dy}$ = 1/2 is the ground pseudospin on the Dy(III) site. The dipolar magnetic coupling can be calculated exactly, while the exchange coupling constant was fitted through comparison of the computed and measured magnetic susceptibilities using the POLY_ANISO program.

Table S12 Exchange energies E (cm^{-1}), the energy difference between each exchange doublets Δ_t (cm^{-1}) and the main values of the g_z for the lowest two exchange doublets of **1** and **4**.

	1			**4**		
	E	Δ_t	g_z	E	Δ_t	g_z
1	0.00	9.74×10^{-7}	38.761	0.00	2.52×10^{-5}	36.425
2	2.21	1.73×10^{-6}	0.000	1.97	3.08×10^{-5}	0.000

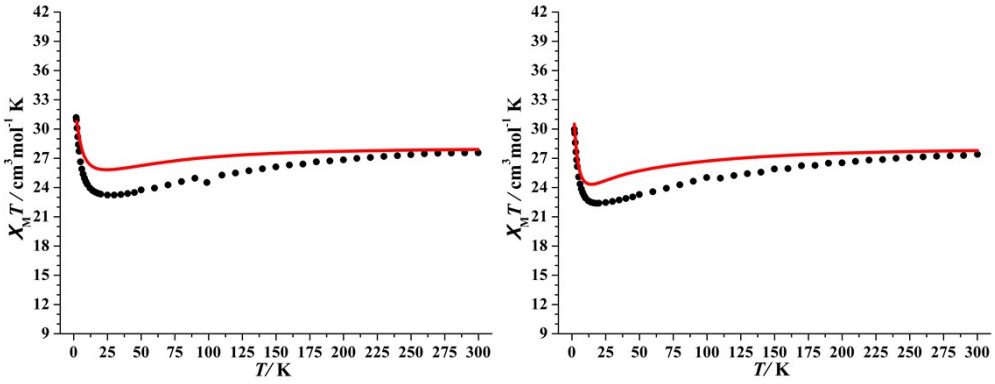

1 **4**

Fig. S17 Calculated (red solid line) and experimental (black circle dot) data of magnetic susceptibility of **1** and **4**. The intermolecular interactions zJ' of **1** and **4** were fitted to −0.02 and −0.01 cm^{-1}, respectively.